University of Pardubice

Faculty of Chemical Technology

Nanoparticles of transition metals oxides with application potential

Bc. Simona Burianová

Bachelor work
2009

Prohlašuji:
Tuto práci jsem vypracovala samostatně. Veškeré literární prameny a informace, které jsem v práci využila, jsou uvedeny v seznamu použité literatury.

Byla jsem seznámena s tím, že se na moji práci vztahují práva a povinnosti vyplývající ze zákona č. 121/2000 Sb. autorský zákon, zejména se skutečností, že Univerzita Pardubice má právo na uzavření licenční smlouvy o užití této práce jako školního díla podle § 60 odst. 1 autorského zákona, a s tím, že pokud dojde k užití této práce mnou nebo bude poskytnuta licence o užití jinému subjektu, je Univerzita Pardubice oprávněna ode mne požadovat přiměřený příspěvek na úhradu nákladů, které na vytvoření díla vynaložila, a to podle okolností až do jejich skutečné výše.

Souhlasím s prezenčním zpřístupněním své práce v Univerzitní knihovně.

V Pardubicích dne 25.6.2009

Simona Burianová

Abstract

We present summary of the most used preparation methods and physical properties of transition metal-based nanoparticles. The physical properties of the nanoparticles can be controlled by particle shape and size that can be affected by conditions of preparation. We mainly described the sol-gel method, co-precipitation and microemulsions method. We summarized physical properties of ZrO_2, TiO_2 and $CoFe_2O_4$ with respect to their possible application.
A series of the cobalt ferrite nanoparticles embedded in silica matrix, obtained by modified sol-gel route, was characterized using X-ray diffraction and ICP-OES. We determined the particle diameter and compared them to the final annealing temperature.

keywords: magnetic nanoparticles, $CoFe_2O_4$, TiO_2, ZrO_2, sol-gel, microemulsion, co-precipitation

Abstrakt

Tato práce se zabývá nejvíce používanými metodami přípravy a fyzikálními vlastnostmi nanočástic přechodných kovů. Fyzikální vlastnosti nanočástic mohou být kontrolovány pomocí velikosti a tvaru částic. Na velikost částic mají vliv podmínky přípravy. Zabývali jsme se především sol-gelovou metodou, ko-precipitací a mikroemulzí a provedli jsme shrnutí fyzikálních vlastností ZrO_2, TiO_2, $CoFe_2O_4$, které jsou důležitým aspektem pro jejich možné budoucí využití.
Vzorky nanočástic kobaltových ferritů zapoudřených v SiO_2 matrici, které byly připraveny pomocí modifikované sol-gelové metody, byly charakterizovány pomocí rentgenové difrakce a ICP-OES. Byla určena velikost částic, která byla porovnána s finální žíhací teplotou.

Klíčová slova: magnetické nanočástice, $CoFe_2O_4$, TiO_2, ZrO_2, sol-gel, mikroemulze, ko-precipitace

Univerzita Pardubice
Fakulta chemicko-technologická
Katedra fyziky
Akademický rok: **2008/2009**

ZADÁNÍ BAKALÁŘSKÉ PRÁCE

(PROJEKTU, UMĚLECKÉHO DÍLA, UMĚLECKÉHO VÝKONU)

Jméno a příjmení: **Simona BURIANOVÁ**

Studijní program: **B2802 Chemie a technická chemie**

Studijní obor: **Chemie a technická chemie**

Název tématu: **Nanočástice oxidů přechodných kovů s aplikačním potenciálem**

Zásady pro vypracování

1. Rešeršní část
vypracování rešerše na téma:
i) příprava malých částic oxidů přechodných kovů chemickými metodami srovnání metod vzhledem ke krystalinitě a disperzi velikosti částic
ii) významné fyzikální vlastnosti nanočástic TiO_2, ZrO_2 a MFe_2O_4 (M = Mg, Co) - potenciální aplikace
2. Experimentální část
i) studium fázového složení, určení strukturních parametrů nanokrystalické fáze a určení velikosti nanokrystalitů pomocí práškové rentgenové difrakce
ii) určení relativního poměru Fe a Co/Mg pomocí ICP (případně EDAX)

Rozsah grafických prací:

Rozsah pracovní zprávy:

Forma zpracování bakalářské práce: **tištěná**

Seznam odborné literatury:

1. **odborné články na téma příprava a magnetismus systémů TiO2, ZrO2, MFe2O4 (M = Mg, Co), zejména nanostruktur**
2. **G. A. Ozin, A.C. Arsenault: Nanochemistry (Cambridge, RSC Publishing, 2006)**
3. **M. Di Ventra, S. Evoy, J. R. Heflin, Jr.: Introduction to nanoscale science and technology (Norwell, Kluwer Academic Publishers, 2004)**

Vedoucí bakalářské práce: **Mgr. Petr Janíček**
Katedra fyziky

Datum zadání bakalářské práce: **26. února 2009**

Termín odevzdání bakalářské práce: **26. června 2009**

L.S.

prof. Ing. Petr Lošťák, DrSc.
děkan

prof. Ing. Slavomír Pirkl, CSc.
vedoucí katedry

V Pardubicích dne 26. února 2009

Contents:

1 Motivations and aims of the work

The research of nano-sized materials is growing in last years due to their large application potential. Their physical properties are mostly very different from the bulk systems because of their small (sub-micron) size. One of the most investigated groups of the nanomaterials are magnetic nanoparticles. It is due to their possible application in biomedicine [1], magnetocaloric devices [2], magnetic recording [3] etc. This class of materials is mostly represented by the oxides of magnetic elements. The physical properties are affected by the particle diameter, which varies according to the method of preparation. My bachelor work is therefore highly motivated with description of the preparation techniques and the physical properties of materials that are suggested for potential application.

The aims of the bachelor work are summarized as follows:

1) Description of the used preparation techniques,
2) Physical properties of the materials and their application,
3) Characterization of the samples by X-ray diffraction and ICP (Ion Coupled Plasma).

The bachelor work is divided into several parts:

It starts with motivation and aims of the work (Chapter 1). In the beginning (Chapter 2), the preparation techniques are described – the sol-gel method that has been used for long time before the scientific`s background was known. Another two well-known methods, co-precipitation and microemulsion, are described as well.

In the next section the physical properties of the three important oxide compounds and their crystal structures are discussed. The TiO_2 and ZrO_2 are useful materials that has been utilized for many decades as white pigments and ceramic material, respectively [4]. Nowadays, they are considered as potential ferromagnetic semiconductors. The $CoFe_2O_4$ is a material with advanced magnetic properties that can be utilized in biomedicine or magnetic recording.

The experimental techniques including preparation, X-ray diffraction and ICP are summarized in Chapter 3.

The experimental part (Chapter 4) of my bachelor work is concentrated on characterization of $CoFe_2O_4$ nanoparticles by X-ray diffraction and ICP. The X-ray diffraction is a powerful method for characterization of sample that has been used for many decades. From this method we can obtain`, beside the phase composition, the particle diameter that plays the crucial role in physical properties of nanoparticles. Finally, conclusions of the presented results are given (Chapter 5).

2 Theoretical part

2.1 Methods of preparation

The most important and used methods are sol-gel, co-precipitation and microemulsion that will be discussed in this chapter in more details. I would like to briefly mention that there are other methods that can be used for preparation. One of another chemical method is hydrothermal process. In hydrothermal synthesis the solvent is brought to temperature well above its boiling point by the increase in pressure. Under this condition a chemical reaction can be performed. Its advantage is in easily dissolution of chemical compounds that would otherwise exhibit very low solubilities under ambient conditions. Moreover, the products are usually crystalline hence do not need postannealing treatment [5]. Other chemical methods are citrate gel or polymer complex.
There are also several physical methods as many types of mechanical milling (vibration mill etc) or mechano-chemical synthesis that can be also used for preparation the nanoparticles. These methods have one significant disadvantage - the product can be contaminated from the milling media and atmosphere.

2.1.1 Sol-gel method

The main part of this section is well described in the references I used [6, 7, 8].

History
Sol-gel processing methods were first used historically for decorative and constructional materials. This method was used very long time before the scientific principles were understood. The origins of this method (using colloids) can be found in the cave paintings at Lascaux in France, dating back 17 000 years. The used pigments were based on iron oxide, carbon and clays, grounded into fine powders, graded by sedimentation and dispersed in water using natural oils as surface active stabilizers. The next development of the idea of sol-gel was in construction materials as concrete (for example 700 BC, Aqueduct Bridge at Jerwan in Iraq), bricks, and plaster or in glazing methods to seal the surfaces of porous clay vessels (China or Egypt, 2000BC). There was no big progress during thousands years till the 19th century. In 1846 Ebelman [9] prepared the first silicon alkoxides by the reaction between silicon tetrachloride and alcohol, that restored the interest in sol-gel chemistry, but for many decades this development had little scientific impact for the development of the sol-gel materials field. One of the first pioneers of this field was W.A. Patrick [10], who in the twenties of 20th century filed many patents for supported catalysts, including the use of sol-gel

methods. This was the beginning of an intensive period of technological development using sol-gel methods, which produced a very large number of patents and many useful materials. There were many publications of using this method for preparation of catalyst materials, ceramic materials, aerogels, fibres etc. The present target for sol-gel physics is preparation of nanocomposites, because all gel products may contain nanoparticles [11]. This plays a big role in development of modern nanotechnology. The main source for scientific information is Journal of Sol-Gel Technology starting in 1993. An important peculiarity of sol gel technologies is the possibility to control the mechanism and kinetics of proceeding materials.

Theory

The sol-gel method involves the production of colloidal suspensions („sols“) which are subsequently converted to viscous gel and thence to solid material. Colloids are suspensions of particles of linear dimension between 1nm and 1 μm. The big advantage of this method is that by changing the reaction conditions as pH, concentration of catalyst, temperature and time of reaction or H_2O/Si molar ratio, the properties and characterization of resulting product can be tuned. The reaction mechanism of sol-gel method can be divided into several steps, which will be now discussed in more details: hydrolysis, condensation, gelation, ageing, drying and densification. It is necessary to point out, that in real systems several of these steps may occur concurrently.

1) Hydrolysis

The general mechanism of hydrolysis reaction can be shown:

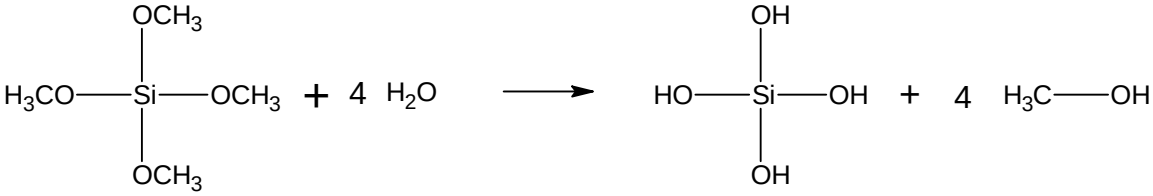

By addition of water the alkoxy groups are replaced by hydroxy groups. This reaction can occur more rapid, if the catalyst (as mineral acid or ammonia) is added. Additionally, it has been observed, that the rate and extent of the hydrolysis reaction is most influenced by the strength and concentration of the acid- or base catalysts. Due to the electronic effects (alkoxy groups are more electrons donating than hydroxy group) the rate trends are different in acid- and base-catalysed process. In the acid-catalyzed reaction, as more alkoxy groups are replaced by hydroxy, the transition state becomes less stabilized and the reaction rate decreases. On the other hand, in base-catalyzed process, as the transition state becomes more stable, the reaction is faster.

Another thing that has to be taken into account is the hydrophobic or hydrophilic character of the precursor. For instance, if we use tetraethoxy silane (TEOS), that is

hydrophobic, we have to add co-solvent (like ethylalcohol) to make the hydrolysis possible.
The molar ratio of Si/H_2O needs more attention, because this ratio influences the reaction rate. In next step condensation, the water is produced, so less water can be used than what arises from stoichiometry conditions. However, if a small amount of water is used, the hydrolysis rate slows down due to the reduced reactant concentration.

2) Condensation

Condensation can be either water condensation or alcohol condensation:

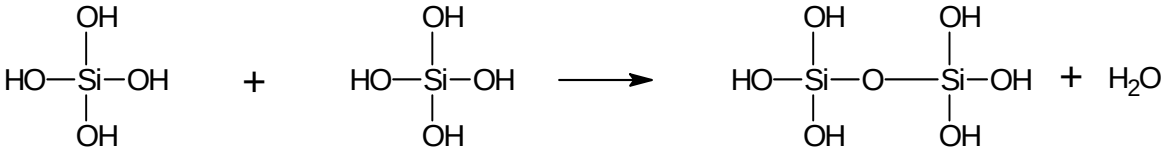

This reaction involves producing of siloxane bonds (≡Si-O -Si≡) from the silanol groups (Si-OH) plus by-products water or alcohol. This reaction could be also acid- or base catalysts. This reaction proceeds via a rapid formation of a charged intermediate by reaction with a proton or hydroxide ion, followed by slow attack of a second neutral silicon species on this intermediate. If we have an acid catalyzed reaction, the first step of the hydrolysis is the fastest, and the product of this first step also undergoes the fastest condensation. The consequence is the producing of linear, open networks. On the other hand under base catalyzed conditions the highly cross-linked large sol particles are produced, that form gels with large pores between the interconnected particles (see Figure 2.1).

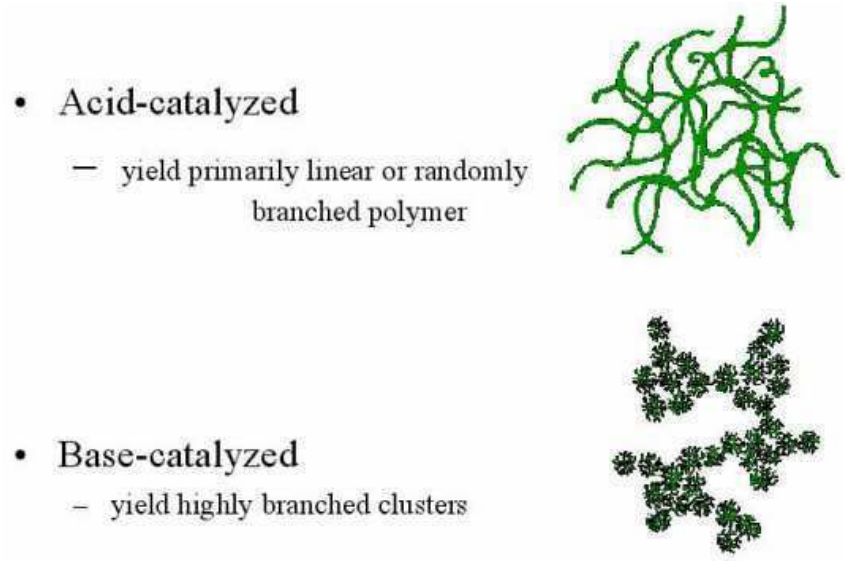

Fig. 2.1 – Gel structure for acid or base catalyzed reactions [7].

3) Gelation

Gelation is the process, where the links are formed among silica sol particles through whole vessel. The mixture has a high viscosity but low elasticity. There is no discrete chemical change at the gel point, only viscosity and then elasticity is rapidly increasing.

4) Ageing

In this time more and more siloxane bonds are creating, that can continue for months for samples at room temperature, the rate depending on pH, temperature and gel composition. The net effect is a stiffening and shrinkage of the sample. The homogeneous gel is gradually changed to transparent shrunken solid monoliths immersed in liquid. This process is known as syneresis. Another process is ripening (the particles join to each other with narrow „necks“). Ageing usually improves the properties of the material.

5) Drying

Drying is the process, where the water or alcohol is loosing firstly due to the syneresis, secondly as evaporation of liquid from the pore structure.

6) Densification

If we would like to produce dense glasses and ceramics from gels, heat treatment is needed. As mentioned above, all of the steps depend on the reaction conditions as pH, temperature etc. Hence, the details of effects of heat treatment depend on previous stages.

Application

Sol-gel method is widely used for preparing the nanocrystals, ceramics and glasses that can be utilized in many technical applications (see Figure 2.2). It is due to the many advantages that this method obtained. Firstly, non-metallic, inorganic solids can be produced and processed at temperatures which are considerably lower than those required in conventional methods. Secondly, the structure and pore size distribution of material can be controlled by the chemical composition of starting material or by the reactions conditions.

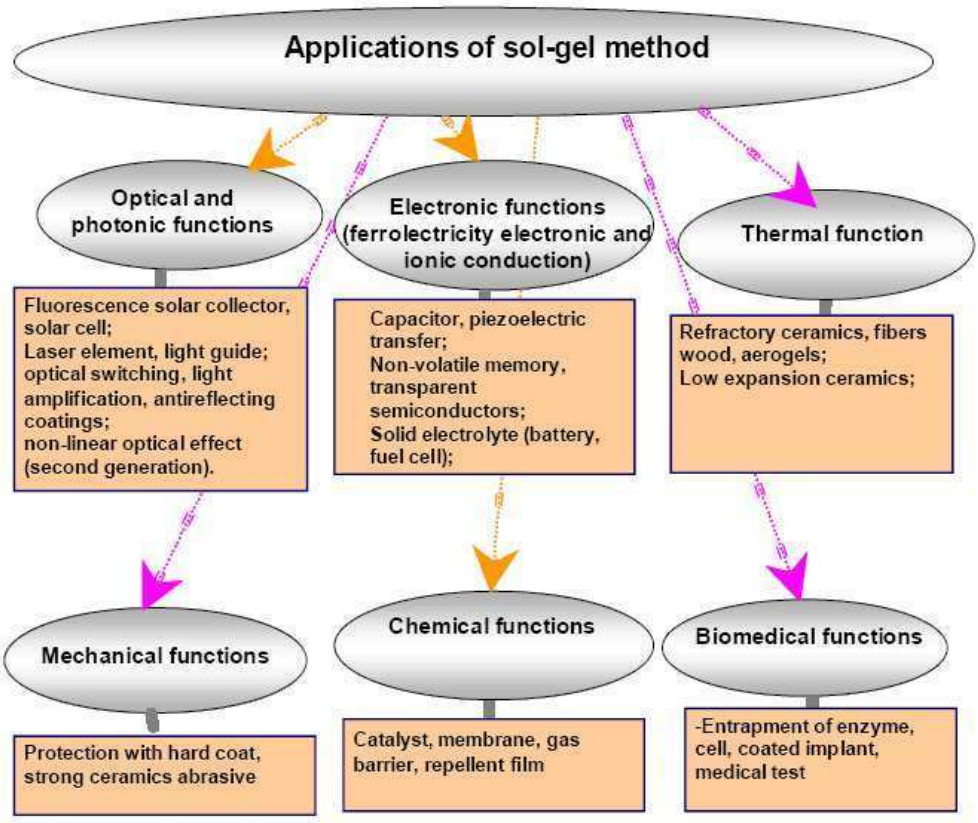

Fig. 2.2 – Application of products that were prepared by sol gel method [8].

2.1.2 Co-precipitation

The useful method for preparation of homogenous and monodisperse nanoparticles is via homogenous precipitation. This method involves the nucleation, growth of the nuclei and the secondary process as coarsening and agglomeration. The nucleation can occur only when the concentration of constituent species reaches critical supersaturation. The high supersaturation guarantees that a large number of small particles will be formed. This necessary condition is usually the result of chemical reaction. Hence, precipitation can be induced by simple addition/exchange reactions, chemical reduction, photoreduction, oxidation and hydrolysis. Generally, chemical reaction is chosen that result in products with low solubility, such that solution quickly reaches supersaturated conditions.

The degree of supersaturation, *S*, for a simple chemical reaction is given by:

$$S = \frac{a_A a_B}{K_{sp}} \tag{1}$$

where a_A and a_B are the activities of the solutes A, B and K_{sp} is the solubility product constant.

As the nucleation begins, there exists an equilibrium critical radius, R^* (depends on degree of supersaturation *S*, temperature *T* and surface tension at the solid-liquid

interface). Nucleated particles with $R>R^*$ will continue to grow, while the others dissolve.

The nuclei can grow uniformly by diffusion of solutes from the solution to their surface until the final size is attained (curve I in Figure 2.3). The growth rate is determined by concentration gradient and temperature. To achieve monodisperzity, these two stages must be separated. To produce nanoparticles, the nucleation process must be relatively fast while the growth process remains relatively slow.

However, uniform particles can be also obtained by multiple nucleation's events with Oswald ripening (curve III in Figure 2.3). Coarsening (Ostwald ripening) is the process, where smaller particles are essentially consumed by larger particles during the growth process.

Another possibility, how to get uniform nanoparticles is by aggregation of smaller subunits (curve II in Figure 2.3). It is due to the thermodynamics that favor the maximization of the surface/volume ratio. Hence, the agglomeration of small particles precipitated from solutions is practically inevitable without using the stabilizers. There are two possibilities, how to stabilize the nanoparticles. The most common is the steric repulsion between particles caused by surfactants or polymers or other organic species bound to the nanoparticle`s surface. Another is electrostatic repulsion (Van der Waals) resulting from the chemisorptions of charged species at the surfaces. These two secondary processes have dramatically effect on the size, morphology and properties of the products (nanoparticles).

More information about this method is in used references [1,5].

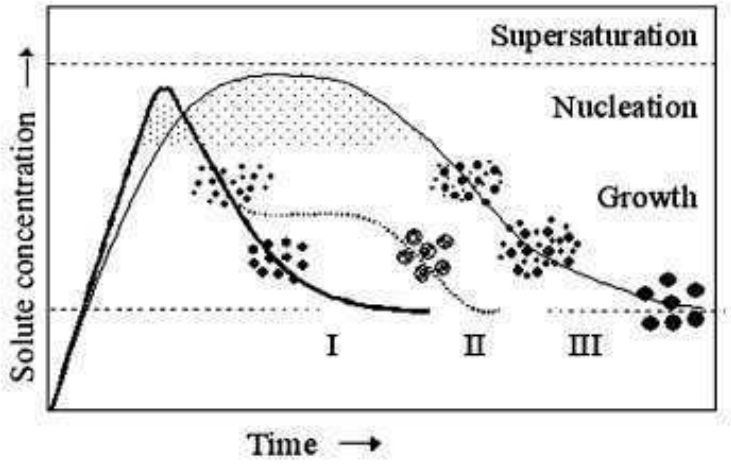

Fig. 2.3 - Formation mechanism of uniform particles in solution: curve I – single nucleation and uniform growth by diffusion; curve II – nucleation, growth and aggregation of smaller subunits; curve III – multiple nucleation events and Ostwald ripening growth [1].

2.1.3 Microemulsions

The microemulsion is one of the useful methods, how can be uniform nanoparticles synthetized [5]. The term micro-emulsion was firstly used by T. P. Hoar and J. H. Schulman in 1943 for a homogenous solution that was produced by the certain combination of water, oil, surfactant and cosurfactant [12]. However it was found out that this mixture cannot be described as solution, because the orientation of surfactant molecules is not random [13]. Surfactants (named after surface-active-agent) are molecules with amphiphilic character because of their composition; they have hydrophilic head and hydrophobic tail. These molecules are able to modify the interfacial properties of the liquids in which they are present. In the solution of water, oil and surfactant the surfactant create a micelle, that is an aggregation of surfactant with the hydrophilic head in contact with water (solution) and the hydrophobic tails close oil in the centre of micelle (in Figure 2.4 it is the hydrophobic oleimicelle). In our case, the surfactant with the cosurfactant creates an inverse micelle through ion-dipole interactions (in Figure 2.5 is this shown as oleophilic hydromicelle). The cosurfactant acts as an electronegative "spacer" that minimalizes repulsions between the positively charged surfactants heads.

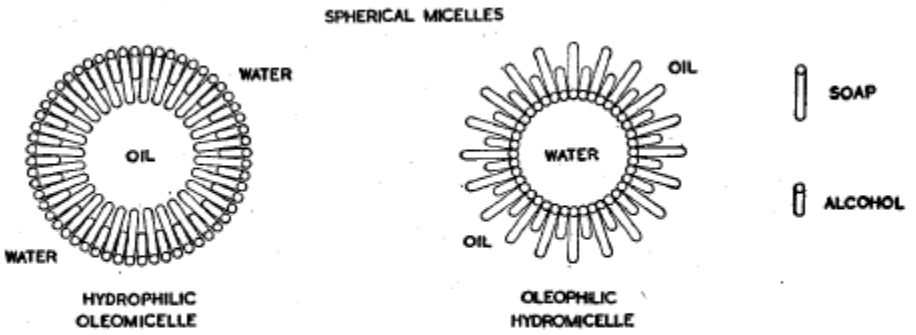

Fig. 2.4 - The illustration of various type of micelle (the left picture shows "normal micelle", the right picture shows inverse micelle) [13].

The creation of this inverse micelle depends on the reaction conditions, mostly on the ratio of using water, oil and surfactant concentration.

As the micelle is small (the radius of micelle mostly depends on ratio of $\frac{[H_2O]}{[S]}$) it performs a Brownian motion, even at room temperature. Hence, there are lots of collisions between two micelles. These two micelles create for a short time (~100 ns) a dimmer. During this lifetime of dimmer, two reverse micelles will exchange the contents of their aqueous cores before uncoupling (see Figure 2.5). This leads to equilibrium distribution of all contents. It is obvious that centre of micelle can be used

as nanoreactor that produce nanoparticles with uniform size and shape. This size of nanoparticles can be controlled by the radius of micelle.

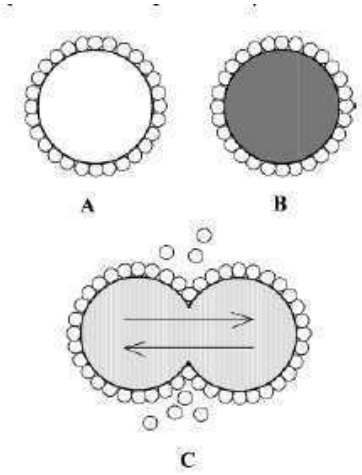

Fig 2.5 - The schema of collision between two reverse micelles A, B with dissimilar cores [5].

2.2 Materials with potential application

2.2.1 Zirconium dioxide (zirconia) - ZrO_2

Zirconium dioxide is a white crystalline oxide of zirconium. Pure zirconia crystallizes in three crystal phases at different temperature. The low-temperature (below 1200°C) phase with a monoclinic crystalline structure, is the most naturally occurring form as the rare mineral baddeleyite (it was named after Joseph Baddeley). The intermediate temperature phase (till 2370°C) has a tetragonal crystalline structure that at higher temperature transforms to the cubic structure that exists till melting point 2680°C. This cubic form, called „cubic zirconia", is rarely found in the nature as mineral tazheranite. Some of physical properties are shown in Table 2.1. These properties mostly depend on type of crystal structure or if the zirconium dioxide is stabilized or not.

Table 2.1: Physical properties of zirconium dioxide:

Density	Thermal conductivity	Molar mass	Boiling point	Refractive index
ρ (g.cm^{-3})	σ (W.m^{-1}.K^{-1})	M_r (g.mol^{-1})	T_B (°C)	n
5.6-6.1	2.7-3	123.2	4300	2.1

Crystal structure

Pure cubic ZrO_2 has the fluorite structure with each metal ion in regular eightfold-coordinated sites having all of the Zr-O bonds of equal length. In the tetragonal phase, the Zr^{4+} ions are located in distorted eightfold coordination environments while, in monoclinic ZrO_2, Zr^{4+} ions are located in sevenfold coordination [14]. The details of crystal structure of these phases are shown in Table 2.2 [15,16] and the pictures of crystal structure are shown in Figure 2.6.

Table 2.2: Crystal information of ZrO_2:

	Monoclinic (baddeleyite)			Tetragonal			Cubic (tazheranite)		
Space group	$P2_1/c$			$P4_2/nmc$			Fm-3m		
Lattice parameters	a (Å)	b (Å)	c (Å)	a (Å)	b (Å)	c (Å)	a (Å)	b (Å)	c (Å)
	5.169	5.232	5.341	3.612	3.612	5.212	5.111	5.111	5.111
	α (°)	β (°)	γ (°)	α (°)	β (°)	γ (°)	α (°)	β (°)	γ (°)
	90	99.25	90	90	90	90	90	90	90

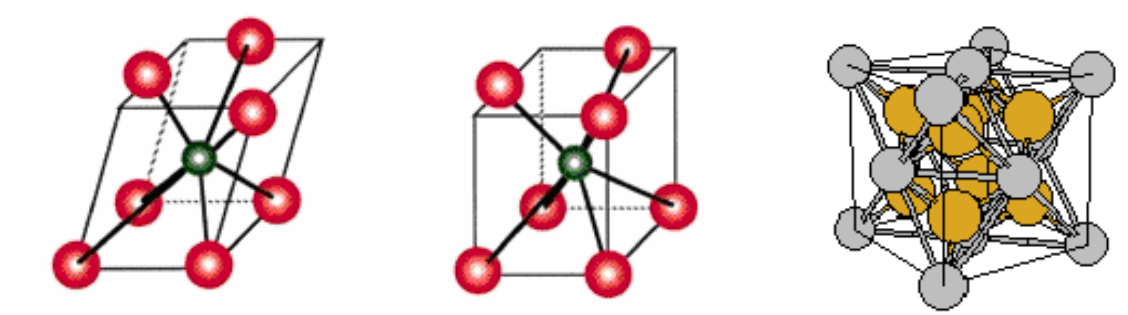

Fig. 2.6 - The crystal phases of zirconium dioxide – in left panel is shown monoclinic structure (baddeleyite), in the middle panel is shown tetragonal phase (red balls are atoms of oxygen, green ball is atom of zirconium). In the right panel is shown cubic phase, where brown balls are atoms of zirconium, and red balls are atoms of oxygen. [17,18].

Applications

In the past the zirconium dioxide was used for showing diapositives because by heating up, ZrO_2 emits an intensive light known as zirkon light [4].

Cubic zirconia is used in jewellery as synthetic substitutes for diamond known as zircon. It is due to the fact, that the cubic form has high refractive index like diamond that also crystallizes in cubic form. Hence, it is difficult to distinguish zirkon from diamond at first sight. The differences between these two jewelleries are in physical properties as thermal conductivity, that is lower for cubic zirconia (diamond is a very good thermal conductor, $\sigma = 900\text{-}2320\ W.m^{-1}.K^{-1}$). Due to this low thermal conductivity, zirconium dioxide is using as thermal barrier coating in diesel engine.

The zirconia is widely used as a ceramic material. It is due to the many favorable physical properties as high melting point, low coefficient of thermal expansion, acido and base resistance. However pure zirconia materials tend to cracking when it is annealed and than repeatedly cooled down. It is due to the fact that the transformation from tetragonal to monoclinic structure is accompanied by a large change in lattice parameters. A consequence of this phase change is a large volume expansion on cooling, which make the fabrication of pure zirconia ceramics impossible. Hence, it is necessary to maintain the cubic crystalline structure at low temperatures. This can be achieved by adding cubic stabilizers as CaO, MgO, Y_2O_3. Cubic stabilized zirconia is a useful refractory and technical ceramic material (as fire-resistant materials – melting crucible) because it does not go through destructive phase transitions during heating and cooling [4].

New possibility of using cubic zirconia is in spintronics devices. Spintronics (spin transport electronics or spin based electronics) is a new paradigm of electronics based on the spin degree of freedom of the electron. In this case the carrier of information is the electron spin that add many advantages as nonvality, increased data processing speed or increased integration densities compared with conventional semiconductor devices. Hence, it is useful to search for materials, that combine properties of the ferromagnet and the semiconductor, such as diluted magnetic semiconductors DMS (alloys in which some atoms are randomly replaced by magnetic atoms) [19]. One of

these promising materials is Mn-stabilized zirconia. It is due to the fact, that it is theoretically predicted, that this material could be magnetic above the room temperature because of the atoms of Mn^{2+} that is magnetic [20]. To prove this experimentally more studies are needed.

2.2.2 Titanium dioxide - TiO_2

Titanium dioxide is widely known material for its many applications that will be discussed later. The pure TiO_2 is colorless, but the natural form contains a small amount of iron that causes the black color of this mineral. The most occuring form in nature is as mineral rutil. The name comes from Latin – rutilus (red) that is because of the red color that can be observed when it is viewed by transmitted light. Rutil has the highest refractive index of any known mineral. Titanium dioxide can be rarely found as anatas or brookite. The both anatas and rutil crystallize in tetragonal structure. The name anatas comes from Greek "anatasis" (extension) because of vertical axis that is much longer than in rutil form. Brookite that was named after the English mineralogist Henry James Brooke is different from the other two mineral because it crystallizes in orthorhombic structure. Hence, it has also different physical properties as no photocatalysist`s activity. Some physical properties of titanium dioxide are shown in Table 2.3.

Table 2.3: Physical properties of titanium dioxide:

Density	Thermal conductivity	Molar mass	Boiling point	Refractive index
ρ (g.cm^{-3})	σ (W.m^{-1}.K^{-1})	M_r (g.mol^{-1})	T_B (°C)	n
4.2	11.7	79.9	2972	2.49-2.61

Crystal structure

In a rutil form every atom of titanium is surrounded by six atoms of oxygen that create a distorted octahedron. Two of them are in a distance 2.01Å from titanium and the remaining four atoms are in distance 1.92Å. Anatas crystallizes in the same structure (tetragonal), it differs from rutil only by the distance of oxygen (two of them lie in the distance 1.95 Å, and the other four in 1.91 Å). In Brookite mineral, every atom of titan is also surrounded by six atoms of oxygen that are not in even distance [4]. The details of these three mostly occurring crystal structures of TiO_2 are shown in Table 2.4 [15] and the pictures are shown in Figures 2.7, 2.8.

At 642°C anatas undergoes an enantiothrophy exchange. These modifications are named anatas α and β. At 915°C anatas and also brookite are transformated to rutil form. The melting point of titanium dioxide is about 1840°C [4].

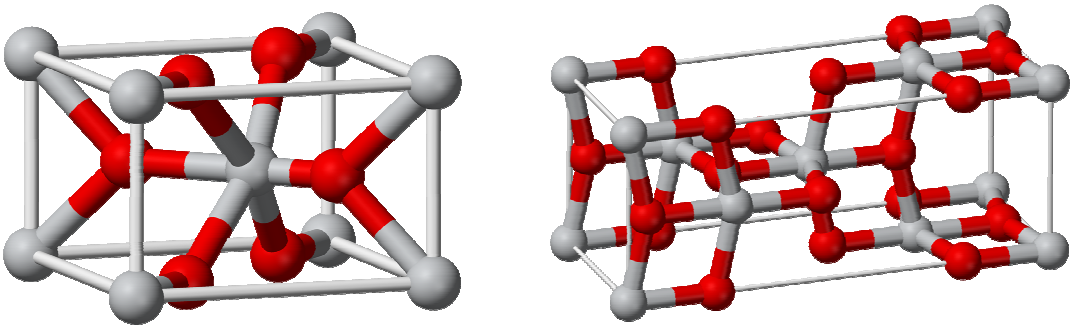

Fig. 2.7 – Images of crystal structures of TiO_2 – in the left panel is shown the rutil, in the right panel is shown anatas. The titanium atoms are grey, the oxygen atoms red [21].

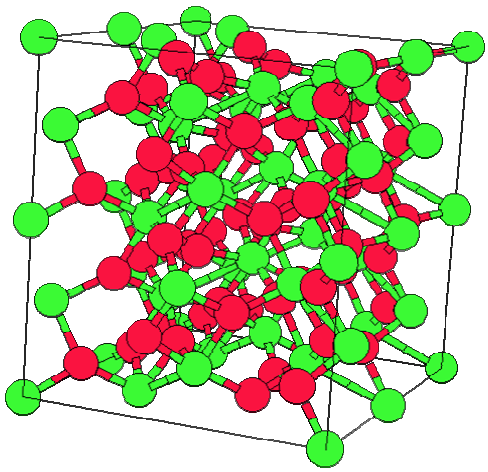

Fig. 2.8 – Image of crystal structure of brookite – green points are oxygen atoms, red points are titanium [18].

Table 2.4: The crystal information of TiO_2:

	Rutil (tetragonal)			Anatas (tetragonal)			Brookite (orthorhombic)		
Space group	$P4_2/mnm$			$I4_1/amd$			Pbca		
Lattice parameters	*a* (Å)	*b* (Å)	*c* (Å)	*a* (Å)	*b* (Å)	*c* (Å)	*a* (Å)	*b* (Å)	*c* (Å)
	4.593	4.593	2.959	3.784	3.784	9.514	9.174	5.449	5.138
	α (°)	β (°)	γ (°)	α (°)	β (°)	γ (°)	α (°)	β (°)	γ (°)
	90	99.25	90	90	90	90	90	90	90

Applications

Titanium dioxide (in anatas or rutil form) is widely used as a white pigment (white titanium) due to its high refractive index (rutil 2.71, anatas 2.53). It has the best covering power from all the white pigments. White titanium is mostly used for fabrication (manufacture) paints, papers, in medicine (pills and tablets), ceramics etc. Its other utilization is in food-processing industry (for example whitening skimmed milk) or as cosmetic products because of UV resistant properties.

The other big field of application of TiO_2 is using it as photocatalyst. This effect was firstly observed by Prof. A. Fujishima in 1972 [22]. He found out that water can be decomposed to oxygen and hydrogen atoms by exposing a titanium oxide electrode in aqueous solution to strong light. This effect has many commercial applications (shown in Figure 2.10). It is widely used as a material for antibacterial tiles or in air-cleaning systems as photocatalyst could decompose materials. The other utilization is in self-cleaning function that is used in side-view mirrors or at exterior materials of buildings (this effect was discovered in 1995 also by Prof. Fujitshima). When glass coated with titanium dioxide is exposed to light, water droplets form a uniform film on the surface - the surface exhibit “superhydrophilicity”. Hence, if oil is present on the surface the water falling on the coated surface penetrates under the oil and removes it easily [23]. This effect is shown in Figure 2.9.

Breaking water into hydrogen and oxygen atom could have another possible application. If the hydrogen atoms are collected, they can be used as a fuel, but the efficiency of this process is by that time relatively small.

The titanium dioxide is also known to be a wide bandgap semiconductor. In last few years there have been researches in using TiO_2 as a spintronic`s device [20] (the details about spintronic were discussed in previous section).

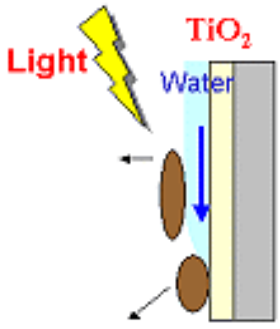

Fig 2.9 – The self-cleaning function of photocatalyst thanks to superhydrophilicity of water. Oil adhered on TiO_2 can be washed with water [23].

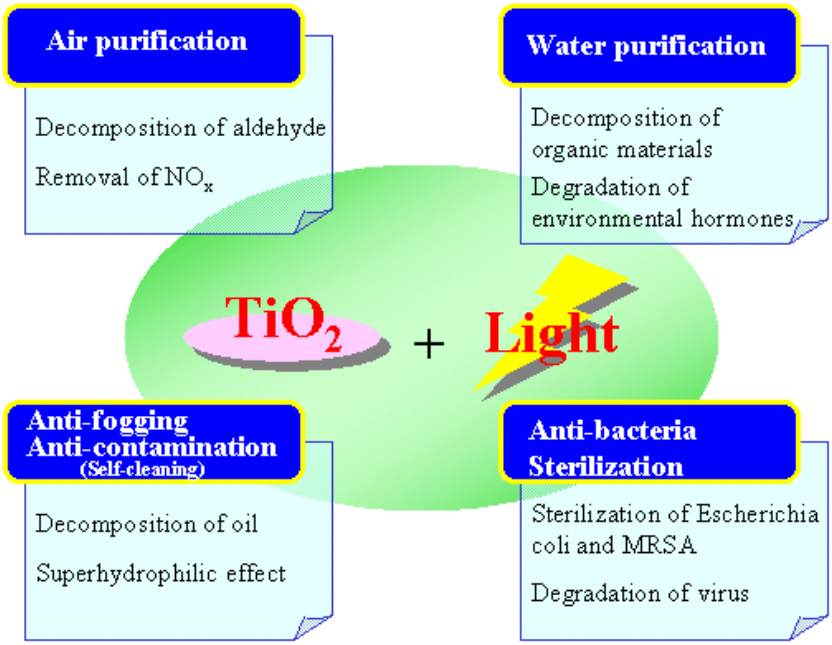

Fig. 2.10 - Fundamental fields in application of photocatalysts [23].

2.2.3 Cobalt ferrite - $CoFe_2O_4$

The cobalt ferrite has been under an intensive research within last years, due to its physical properties that is suggested to be utilized in many technological fields that will be discussed later. This compound has to be prepared in laboratory, because it does not occurring in nature as a mineral.

Crystal structure

Cobalt ferrite belongs to the group of spinels. This structure is named after the compound spinel $MgAl_2O_4$. The general formulation can be written as $A^{2+}B^{3+}{}_2O^{2-}{}_4$, where A, B are metals. The ideal spinel structure consists of cubic close packing of the oxygen ions with the interstitial sites partially filled with the metal ions. The structure is cubic (space group Fd-3m). The metal ions lie in tetrahedral (A) and octahedral (B) sites with the oxygen in the center (see Figure 2.11). The occupation of A and B sites is highly dependent on the kind of metal ions and his charge factor, because the tetrahedral points are smaller then octahedral. There are two mainly possibilities, how to occupy these sites:

a) normal structure

In this type of structure the B^{3+} ions occupy the octahedral site, but usually don't occupy all these positions, so the A^{2+} ions occupy the rest of the octahedral sites and the tetrahedral sites. Example of this structure is $MnFe_2O_4$ or $MgAl_2O_4$.

b) Inverse structure

This presents the inverse distribution of cations. Hence, the tetrahedral sites are occupied by B^{3+} ions and the octahedral sites are occupied by A^{2+} and B^{3+} ions. The most known represent is the magnetite Fe_3O_4 (can be written as $(Fe^{3+})[Fe^{3+}Fe^{2+}]O_4$). The cobalt ferrite is a representative of this type of structure [24].

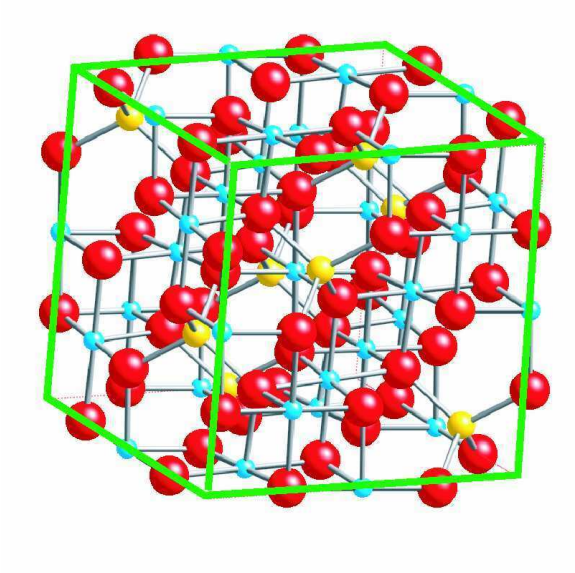

Fig. - 2.11 - The image of the spinel crystal structure – red balls are atoms of oxygen, yellow are tetrahedral sites and blue balls (points) are octahedral sites. In the case of cobalt ferrite, yellow balls are Fe^{3+} ions, and blue balls are Co^{2+} and Fe^{3+}.

As it was mentioned before the crystal structure is cubic with the lattice parameter *a=8.4Å*. The space group is Fd-3m. The positions of atoms in unit cell are written in Table 2.5 [25]. Atoms of Co^{2+} and Fe^{3+} occupy special sites (can be seen from the "special numbers" of fraction coordinates ¼, ½), while oxygen atoms occupy general positions. The positions of oxygen that is shown in Table 2.5 are known from experiments and are for every sample different.

Table 2.5: Fraction coordinates for ions in the $CoFe_2O_4$:

ion	x/a	y/b	z/c
Co^{2+}	0.125	0.125	0.125
Fe^{3+}	0.5	0.5	0.5
O^{2-}	0.23	0.23	0.23

Application

The spinel ferrite nanoparticles are used for various technological applications due to their magnetic properties. The cobalt ferrite nanoparticles have a large magnetic anisotropy that can be utilized in magnetic recording [26]. The magnetocrystalline anisotropy can be simply explained that the crystal possesses a magnetic easy axis and a hard axis. Along certain crystallographic directions it is easy to magnetize the crystal, along others it is harder. Hence, if the material shows a large magnetic anisotropy, we can magnetize it easily in one direction. In magnetic recording the carrier of information is magnetic moment and it is important to not loose this information by magnetize the material in different direction. Another field of utilization is in the production of isotropic permanent magnets because cobalt ferrite shows a reasonable saturation magnetization and high coercivity.

In last few years there has been big research in field of using magnetic ferrite nanoparticle in biomedicine (for example drugs delivery or hyperthermia [1]). The advantage of magnetic nanoparticles is due to their small size that is comparable with the size of biomolecules (as a virus, a protein or a gene). Secondly, because these particles are magnetic, they can be manipulated by an external magnetic field. The idea of hyperthermia is that the particle is injected in the target region (for example the cancer cells). When the magnetic field is applied the particles is heating up to the temperature about 44°C and could damage the surrounding cells.

The concept of delivering the drugs or antibodies was first suggested by Freeman in 1960 [27]. It is based on transporting of the magnetic nanoparticles through the vascular system and concentrating them at the particular point in the body with the aids of magnetic fields. The significant advantage of this method is in targeting of the specifical location in the body, hence the side effects are reduced (minimalizing the concentration of the drugs in nottarget sites) [28].

3 Experimental details

3.1 Preparation

The four samples of $CoFe_2O_4$ encapsulated in SiO_2 matrice were prepared by Holec by the innovative sol-gel method [29]. The precursor is shown in Figure 3.1.

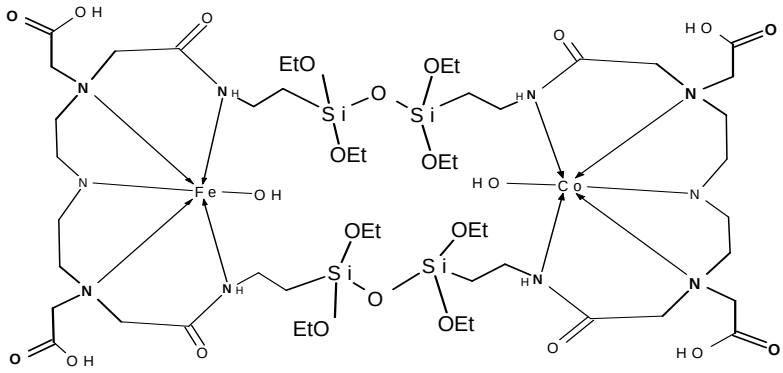

Figure 3.1 - The precursor, that was after the preparation annealed at various temperatures.

After the whole process the materials were annealing at the given temperature (step 1°C/min), all 4 samples are labelled by the number of this temperature (this mean, that the sample Co_800 was annealed at 800°C).

3.2 Powder X-ray diffraction

The powder X-ray diffraction is a convenient method, how can be the crystal structure of the sample characterized. This technique is based on observing the intensity of interfering waves as a function of the diffraction angle. The condition of the constructive interference (the phase shift must be a multiple to 2π – see Figure 3.2) can be expressed by Bragg's law:

$$2d_{hkl}\sin\Theta = \lambda \tag{2}$$

where d_{hkl} is the spacing between the planes in the atomic lattice, Θ is the angle between the incident ray and the scattering planes and λ is the wavelength of X-rays.
From this equation the crystal structure (lattice parameters) could be in special case easily obtained. For instance for cubic lattice, the lattice parameter *a* can be determined from equation:

$$\frac{1}{d^2{}_{hkl}} = \frac{h^2 + k^2 + l^2}{a^2} \tag{3}$$

where *h, k, l* are Miller indices.

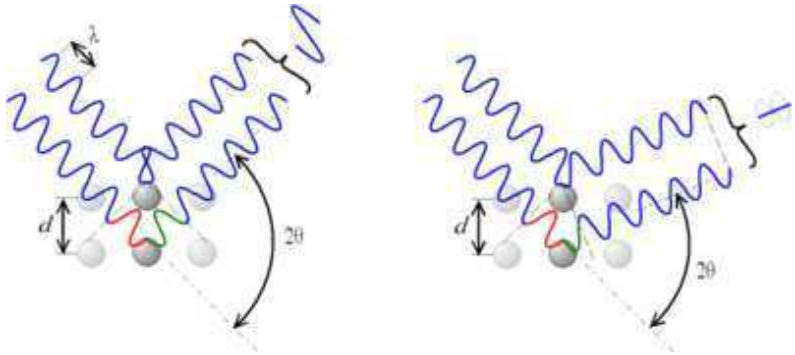

Fig 3.2 - In the left picture the constructive interference is shown, in the right picture destructive interference is shown according to 2Θ deviation [30].

Each material has its unique X-ray powder pattern hence this method could be used for identification of unknown samples by comparing the diffraction pattern to the patterns collected in a database (e.g. Powder Diffraction File). Using the known lattice parameters and fraction coordinates, the data can be fitted by the Rietveld method to obtain exacts crystallographic parameters of the sample.

For calculation particle diameter, it is necessary to known the instrumental resolution function, because this function affects the width of peaks. The resolution function is determined by fitting data of standard sample LaB_6 that were measured by the same diffractometer. The program Fullprof fits data with Voigt function that is convolution of Lorentzian and Gaussian:

$$V(x) = L(x) \otimes G(x) = \int_{-\infty}^{\infty} L(x-u)G(u)du \tag{4}$$

where *L(x)* and *G(x)* have different FWHM (full width in half maximum) H_L, H_G respectively.

$$G(x) = a_G \exp(-b_G x^2) \tag{5}$$

$$L(x) = \frac{a_L}{1 + b_L x^2} \tag{6}$$

where a_G, b_G, a_L, b_L are constants that depend on FWHM of the peak.

From this fitting we can get parameters H_L, H_G and the position of peaks that can be then utilized as knowing resolution function.

If this resolution function is known, the X-ray diffraction can be then used to determine the microstructural effects of the sample as small crystallite sizes or micro-strains. The volume-averaged apparent size of the crystallites in the direction normal to the scattering planes can be calculated from the Scherrer formula:

$$d = \frac{\lambda}{\beta \cos\Theta} \tag{7}$$

where $\beta = \frac{A}{I_0}$ is the integral breadth (*A* is the space under the peak and I_0 is the maximum of the intensity).

The quality of agreement between observed and calculated profiles is measured by set of nowadays-conventional factors. There can be calculated several these factors, but in the output file only two factors are brought out. The Bragg factor R_B and the crystallographic R_F factor:

$$R_B = 100 \frac{\sum_h \left| {}'I_{obs,h}{}' - I_{calc,h} \right|}{\sum_h \left| {}'I_{obs,h}{}' \right|} \quad (8),$$

$$R_F = 100 \frac{\sum_h \left| {}'F_{obs,h}{}' - F_{calc,h} \right|}{\sum_h \left| {}'F_{obs,h}{}' \right|} \quad (9)$$

where '$I_{obs,h}$' is the observed intensity at the point, that contribute to reflection h, $I_{calc,h}$ is calculated intensity, '$F_{obs,h}$', $F_{calc,h}$ are the structural factors with same meaning of indices.

All these mentioned calculations can be done by program Fullprof. More information about this program is in [31] and about X-ray diffraction is in [32].

The X-ray data were collected using the Bruker diffractometer AXS GmbH with the Cu-K_α beam. The X-ray diffraction patterns were collected in the 2Θ range: 10° - 80° with a step of 0.05° for all samples.

3.3 ICP (Inductively Coupled Plasma Spectroscopy)

This method is used to detect trace metals from the samples that are introduced in liquid form for analysis. It consists of the ICP and the spectrometer, which can be optical (ICP-OES) or mass spectrometer (ICP-MS). Argon gas is used for creating plasma of temperature about 7000-8000K by the magnetic field. The sample is atomized by atomizer and given directly inside the plasma flame. Here, at the high temperature, all elements become thermally excited. These excited atoms emit light at their characteristic wavelengths that is collected by the optical spectrometer. The intensity of emitting light is proportional to concentration of the element in the sample.

If we have the ICP-MS, the ICP is used to create charge ions, that are then transfer to the mass spectrometer, where the ions are separated on the basis of their mass-charge ratio. The intensity of ion signal in detector is then also proportional to the concentration.

The concentrations of Co and Fe in our samples were found out using the ICP-OES Integra XL2, GBC, Australia. This analysis was done in Institute of environmental and chemical engineering, Faculty of chemical technology, University of Pardubice.

Samples had to be prepared in liquid form. Samples were dissolved in 4 ml nitric acid and 1 ml hydrochloric acid at 200°C for ten minutes. Then boric acid was added and the mixture was heated at 200°C for another 10 minutes. After this process samples are dissociated and can be injected into the ICP. All samples are encapsulated in SiO_2

matrice. For not counting of this matrice, only the samples with SiO_2 were firstly prepared and measured. This measurement was then counted out as a background.

4 Results and discussion

4.1 Phase analysis

The measured X-ray patterns for samples Co_800, Co_ 1000 is plotted in Figure 4.1, 4.2 respectively with the position of constructively diffraction for $CoFe_2O_4$ (other two samples are in appendix - Figures A.1, A.2). These positions were found in the PDF-4 database. As we can see, positions of our diffraction peaks are in good agreement with the expected one for cobalt ferrite structure. There are no other peaks hence we can suppose that the samples are only single-phase. At the first sight all peaks are very broad as it was expected because of the nanometer size of particles.
It is obvious that with the increasing temperature the intensity of peaks is increasing. It is due to the fact that with the increasing annealing temperature the diameters of particles are increasing and crystallinity of sample is improving, hence there is better diffraction. The peaks are little asymmetric that reflect the strain in the samples.
The first high and broad peak (located about 22°) is thanks to presence of amorphous SiO_2 matrice.

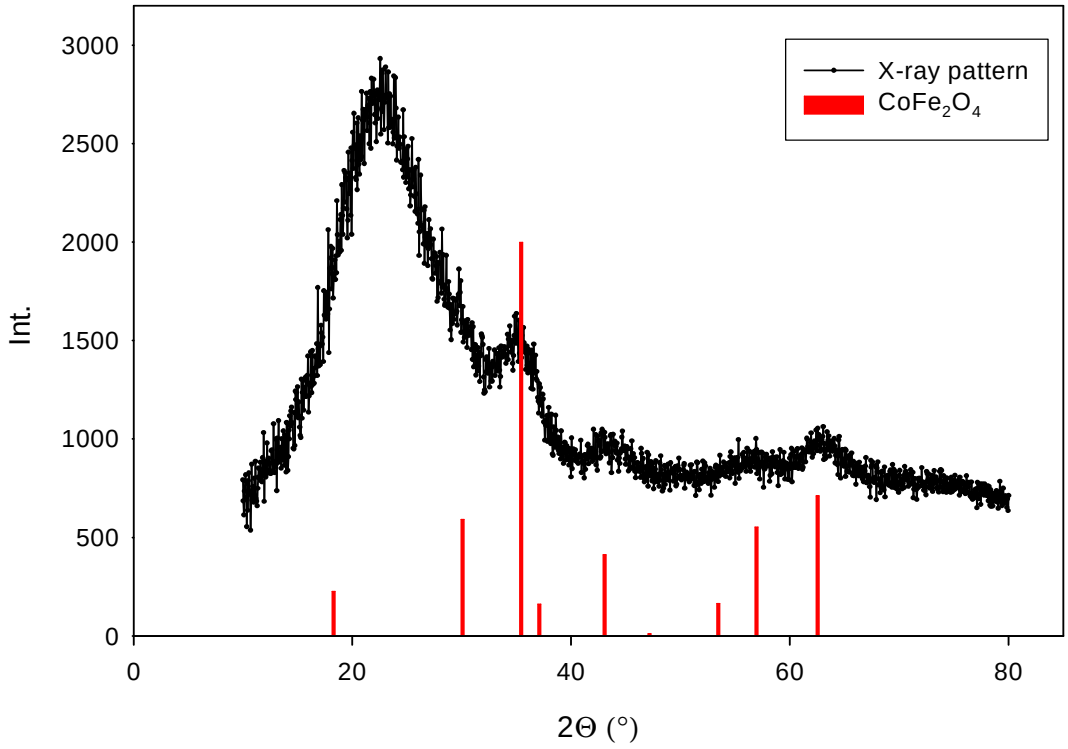

Fig 4.1 – X-Ray diffraction pattern for sample Co_800. The red bars are position of constructively diffraction for $CoFe_2O_4$.

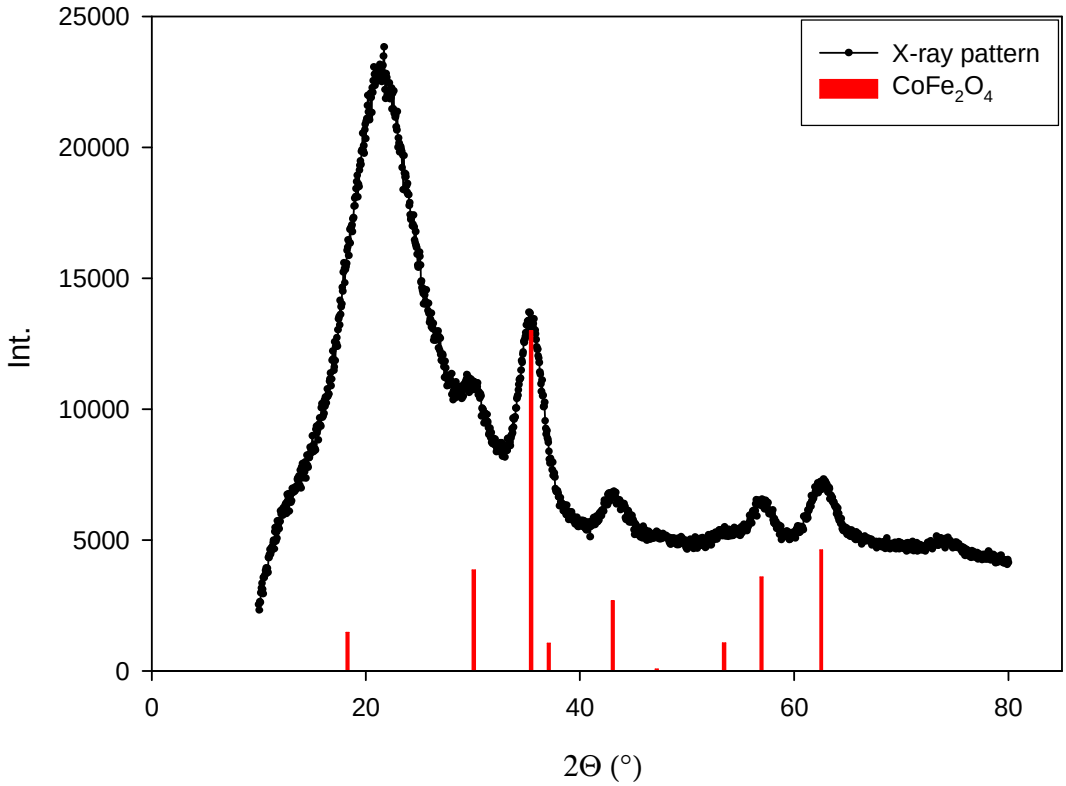

Fig 4.2 – X-Ray diffraction pattern for sample Co_1000. The red bars are position of constructively diffraction for $CoFe_2O_4$.

4.2 Rietvield refinement

The crystal structure of $CoFe_2O_4$ that was used for calculation by Rietveld method was in detail discussed in chapter 2.2.3. The occupancies of atoms were fixed from the stoichiometry. The lattice parameters and fraction coordinates of oxygen atom that were obtained from Rietveld refinement are shown in Table 4.1, 4.2 respectively. Because of the difficult calculation, the peaks of SiO_2 matrice were not included in data that were used in Rietveld refinement. The comparison of the observed and calculated X-ray patterns for samples Co_800 and Co_1000 are shown in Figure 4.3, 4.4 respectively (another two samples are in appendix Figures A.3, A.4).

From the measured data of the standard sample of LaB_6 we found out the resolution function of diffractometer. The particle diameters of all 4 samples were then calculated using program Fullprof from Scherrer formula (mentioned in chapter 3.2). The deviations of the calculated data from measured data are shown in Table 4.1 as the Bragg factor R_B and crystallographic factor R_F. These factors are small (<10) that can reflex good fit. However, particle diameters are only estimative because of the broad peaks and small intensities. For better calculation the longer time of measuring is

needed. This is obvious from the higher Bragg factors of samples Co_1000, Co_1100 that have better diffraction patterns.

Our calculations confirmed that with the increasing annealing temperature the particle diameter is increasing too. There are visible difference between particles that were annealing at temperature 900°C and 1000°C. The fraction coordinates (Table 4.2) for oxygen atoms and lattice parameters *a* are increasing with increasing temperature.

Table 4.1.: Lattice parameter and diameters of samples:

sample	*a* (Å)	*d* (nm)	R_B	R_F
Co_800	8.164(6)	1.6	3.50	2.63
Co_900	8.290(1)	1.7	2.62	2.99
Co_1000	8.359(1)	2.9	9.57	8.10
Co_1100	8.365(9)	3.1	10.7	9.19

Table 4.2: Fraction coordinates for oxygen atom in all samples:

sample	x/a	y/b	z/c
Co_800	0.22(8)	0.22(8)	0.22(8)
Co_900	0.22(9)	0.22(9)	0.22(9)
Co_1000	0.23(1)	0.23(1)	0.23(1)
Co_1100	0.23(0)	0.23(0)	0.23(0)

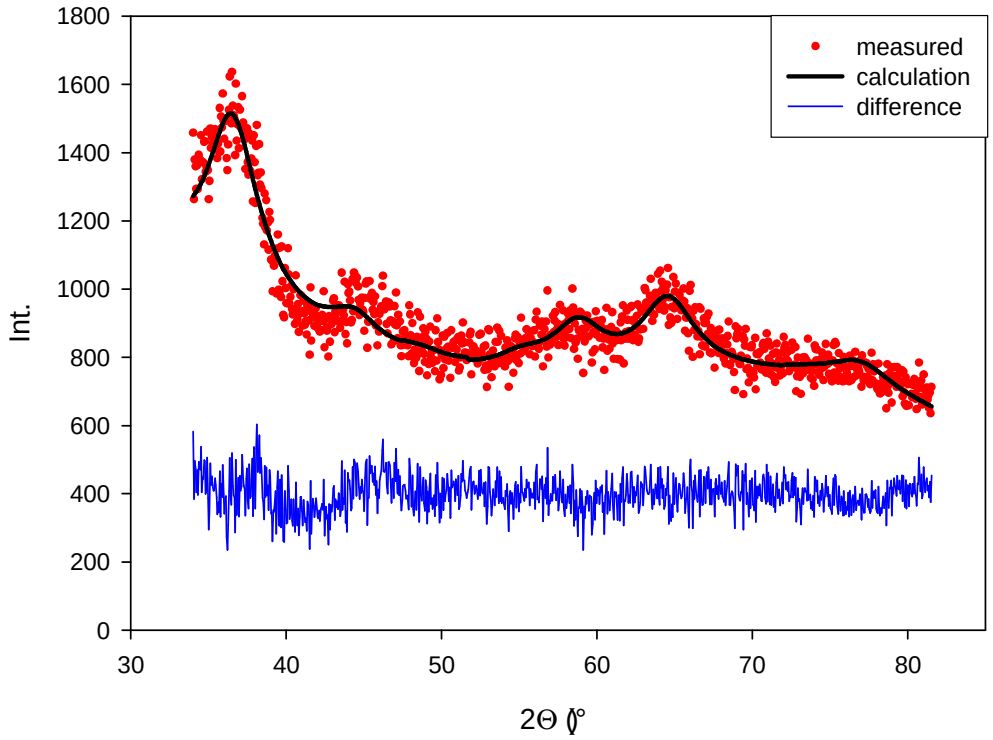

Fig 4.3 – X-Ray diffraction pattern for sample Co_800. The blue line shows the difference between the measured and calculated data.

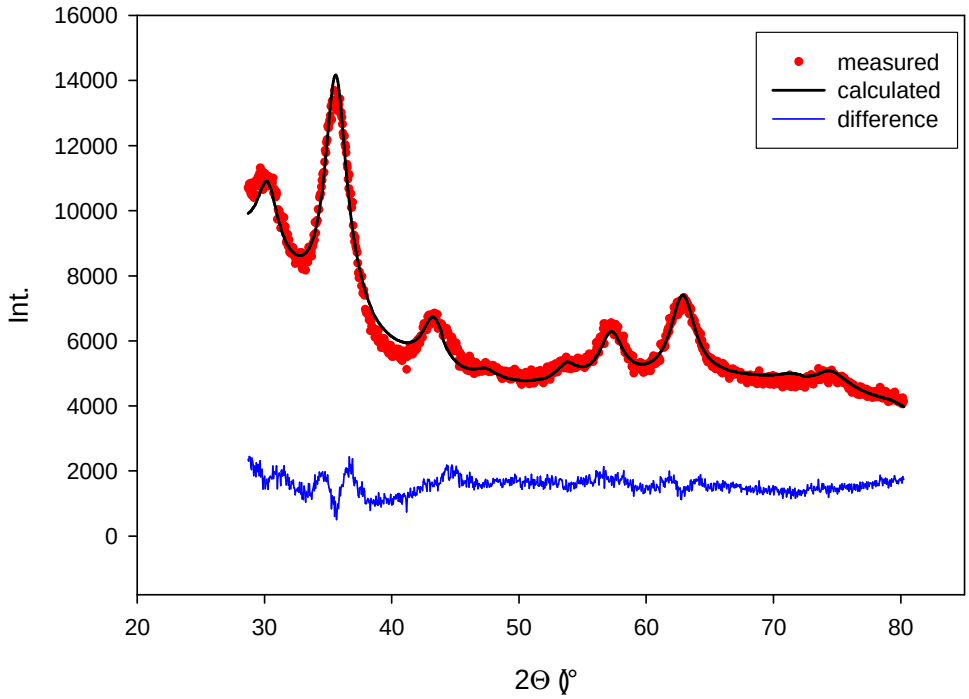

Fig 4.4 – X-Ray diffraction pattern for sample Co_1000. The blue line shows the difference between the measured and calculated data.

4.3 ICP

In Table 4.3 is the measured concentration of iron and cobalt in our samples by the method ICP. As we can see, for all samples there is a good agreement with the demanded stoichiometry. The uncertainty of this method is about 10%.

Table 4.3: The concentration of Fe and Co:

Sample	Fe (%)	Co (%)	Fe/Co
Co_800	4.441	2.320	1.914
Co_900	5.079	2.622	1.937
Co_1000	4.727	2.472	1.912
Co_1100	4.812	2.486	1.936

5 Conclusions

We summarized the most used preparation methods of the nanoparticles. The experimental conditions of the preparation affect the final products, especially their crystallinity and particle diameters. In the sol-gel method, the change of the particle diameters can be adjusted by changing the pH, temperature, molar ratio of concentration Si/H_2O and a kind of catalysis. In the microemulsion method, the size of particle depends on size of created micelle that can be affected by ratio of the concentration H_2O/surfactant. The co- precipitation is useful method for preparation of larger amounts of particles those size depends on reaction mechanism.

We have presented an overview of three possible candidates of nanoparticles for future utilization. We have briefly summarized their crystal structures and their nowadays application (mostly as a bulk material) in our world. We have also sketched their possible application in future. The TiO_2 and ZrO_2 are possible candidates for spintronics applications. The $CoFe_2O_4$ is an excellent candidate for utilization in biomedicine or in magnetic recording.

We have characterized four samples of $CoFe_2O_4$ in silica matrix by X-ray diffraction and ICP method. By matching positions of the diffraction peaks in our $CoFe_2O_4$ nanocomposites to those for $CoFe_2O_4$ spinel phase in the PDF-4 database we found out that our samples are single-phases with the spinel structure. From the Rietveld refinement, we have determined the lattice parameters and using Scherrer formula we calculated the mean particle diameter for all samples. We confirmed that with increasing annealing temperature the particle diameter is increasing from 1.6nm to 3.1nm and the lattice parameters are increasing too. From ICP we found out that the ratio of Fe/Co is in a good agreement with the demanded stoichiometry.

6 References

[1] P. Tartaj, M. P. Morales, S. Veintemillas-Verdaques, T. Gonzales-Carreno, C.J. Serna: *Synthesis, properties and biomedical applications of magnetic nanoparticles*, Handbook of magnetic naterials (2006), **16**, 403-483

[2] S. Harihan, J. Gass: Superparamagnetism and MCE effect in functional magnetic nanostructures, Rev. Adv. Mater. Sci (2005), **10**, 398-402

[3] C. N. Chinnasany, B. Jeyadevan, O. Perales-Perez, K. Shinoda, K. Tohji, A. Kasuya, Nanotech (2003), **3**, 134

[4] H. Remy: Anorganická chemie II. díl, Státní nakladatelství technické literatury, Praha (1962)

[5] B. L. Cushing, V. L. Kolesnichenko, Ch. J. O'Connor: *Recent advances in the Liquid/Phase Syntheses of inorganic nanoparticles*, Chem. Rev., (2004), **104**, 3893

[6] John D. Wright, Nico A. J. M. Sommerdijk: Sol-Gel Materials Chemistry and Applications, CRC Press (2001)

[7] http://www.solgel.com/educational/educframe.htm

[8] Y. Dimitriev, Y. Ivanova, R. Iordanova: *History of sol-gel science and technology*, Journal of the University of chemical technology and metallurgy, 43, 2, 2008, 181-192

[9] J.J. Ebelman, Ann. Chim. Phys. (1846), **16**, 129

[10] W.A.Patrick, "Silica gel and process of making same" U.S. Patent 1,297,724 (1919)

[11] S. Sakka: Sol-Gel technology as reflected in Journal of Sol-Gel Science and technology, J. Sol-Gel Sci Technol (2003), **26**, 29

[12] T. P. Hoar, J. H. Schulman, Nature (1943), **52**, 102

[13] J. H. Schulman, D. P. Riley: *X-ray investigation of the structure of transparent oil-water disperse system I.*, J. Colloid. Sci. (1948), **3**, 383

[14] S. Ostanin, A.J.Craven etc: Electron *energy-loss near-edge shape as a probe to investigate the stabilization of yttria-stabilized zirconia*, Phys. Rev. B (2002), **65**, 224109

[15] crystallographic database for mineral - http://database.iem.ac.ru/mincryst

[16] database PDF-4

[17]http://biomed.brown.edu/Courses/BI108/BI108_2007_Groups/group05/pages/saint_gobain_desmarquest.html

[18] http://cst-www.nrl.navy.mil/lattice

[19] S.A.Wolf, et al.: *Spintronics: A Spin-Based Electronics vision for the future*, Science (2001) **294**, 1488

[20] S. Ostanin, A. Ernts et al: *Mn-stabilized Zirconia: From imitation diamonds to a new-potential high- T_C ferromagnetic spintronics material*, Phys. Rev. Lett. (2007), **98**, 016101

[21] http://en.wikipedia.org/wiki/Titanium_dioxide

[22] A. Fujishima, K. Honda: *Electrochemical photolysis of water at a semiconductor electrode*, Nature (1972), **238**, 37-38
[23] A. Fujishima*: Discovery and applications of photocatlysis – Creating and comfortable future by making use of light energy*, Japan Nanonet bulletin (2005), **44**
[24] G. Subias, J. Garcia, M. G. Proietti et all: *X-ray resonant scattering of (004n+2) forbidden reflections in spinel ferrites*, Phys. Rev. B (2004), **70**, 155105.
[25] International tables for X-ray crystallography, Birmigham, England (1969)
[26] M. Grigorova, H.J. Blythe, V. Blaskov et all: *Magnetic properties and Mossbauer spectra of nanosized $CoFe_2O_4$ powder*, J. Magn. Magn. Mater. (1998), **183**, 163-172
[27] M.W. Freeman, A. Arrott, J.H.L. Watson: *Magnetism in medicine*, J. Appl. Phys. (1960), **31**, S404
[28] M. Arruebo, R. Fernandez-Pachero, M. Ricardo Iberra, J. Santamaría: *Magnetic nanoparticles for drug delivery*, Nanotoday (2007), **2**, 22-32
[29] P. Brazda, D. Niznasky, J-L. Rehspringer, J. Poltierova-Vejpravova*: Novel sol-gel method for preparation of high concentration ε-Fe_2O_3/SiO_2 nanocomposite*, J. Sol-Gel Sci Technol (2009), **51**, 78-83,
[30] http://en.wikipedia.org/wiki/Bragg's_law
[31] J. Rodríguez-Carvajal: An introduction to the program Fullprof (2000)
[32] V. Valvoda, M. Polcarová, P. Lukáč: Základy strukturní analýzy, Karolinum Praha (1992)

7 Appendix A

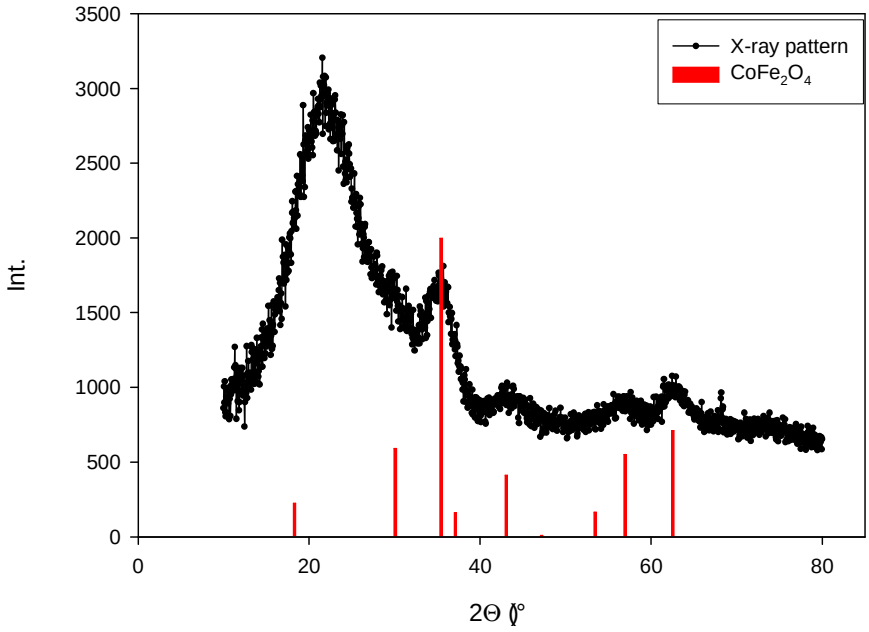

Fig A.1– X-Ray diffraction pattern for sample Co_900. The red bars are position of constructively diffraction for $CoFe_2O_4$.

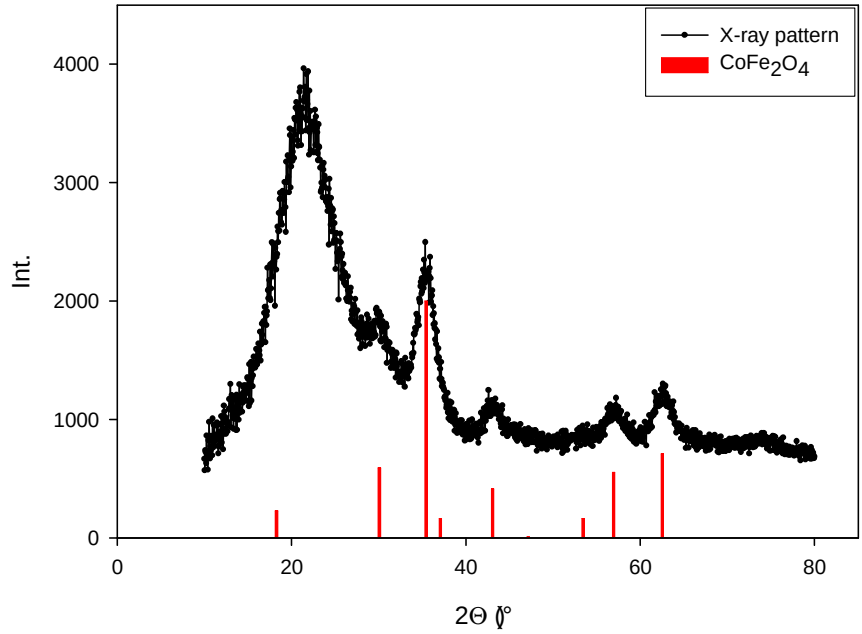

Fig A.2– X-Ray diffraction pattern for sample Co_1100. The red bars are position of constructively diffraction for $CoFe_2O_4$.

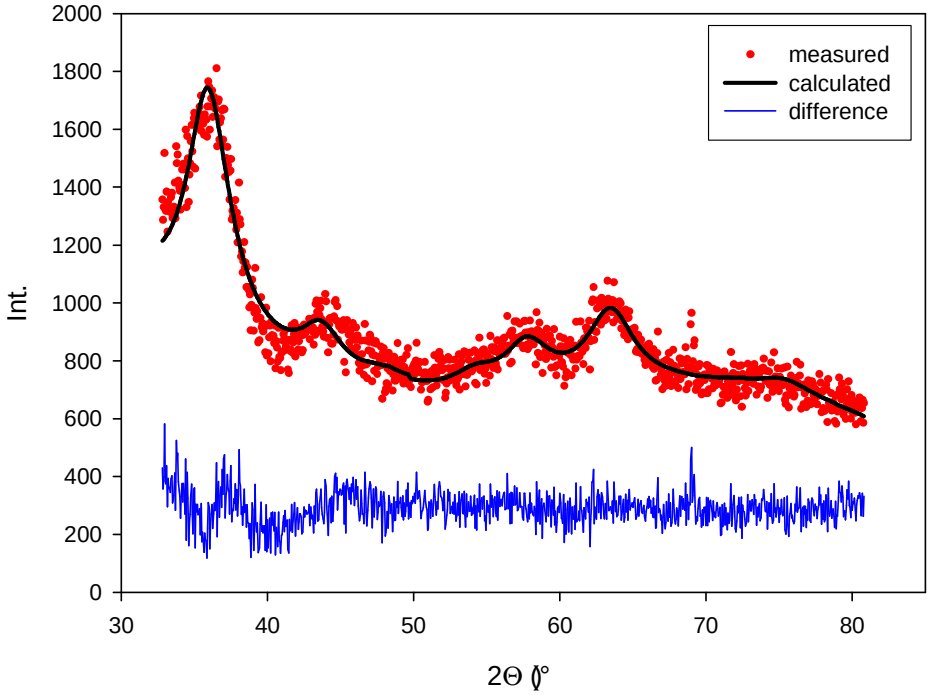

Fig. A.3 – X-Ray diffraction pattern for sample Co_900. The blue line shows the difference between the measured and calculated data.

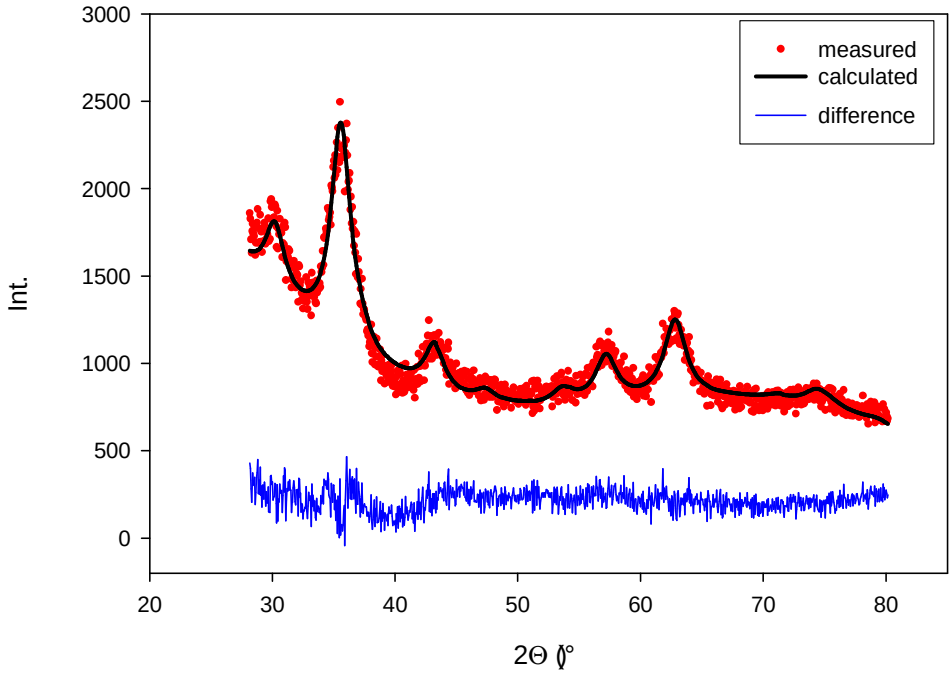

Fig. A.4 – X-Ray diffraction pattern for sample Co_1100. The blue line shows the difference between the measured and calculated data.